Tesi doctoral presentada per En/Na

Marc PERA TITUS

amb el títol

"Preparation, characterization and modeling of zeolite NaA membranes for the pervaporation dehydration of alcohol mixtures"

per a l'obtenció del títol de Doctor/a en

QUÍMICA

Barcelona, 29 de maig del 2006

Facultat de Química
Departament d'Enginyeria Química

UNIVERSITAT DE BARCELONA

APPENDIX A

DETERMINATION OF MOLAR ADSORPTION LOADINGS FROM EXPERIMENTAL BREAKTHROUGH CURVES

The procedure to determine the total amount of a generic species **i** (water or ethanol) retained per kg of zeolite A from a normalized adsorption breakthrough curve is explained in detail below. The calculation process is illustrated for a experiment carried out at 1.48 kPa water vapor pressure, 393 K and ~3 hours of experiment (see Figure A.1). In general terms, the procedure consists of the calculation of the difference between the amount of species **i** (pure water in the example) that is fed to the reactor and the amount that is not retained during the experimental time, both of which can be evaluated, respectively, from normalized blank and adsorption breakthrough curves, as follows:

1. Calculation of the amount of species **i** that is not retained in the bed during the experimental time. As the ordinate of the adsorption breakthrough curve corresponds to the ratio between the signals of species **i** at the outlet and inlet of the reactor measured by the mass spectrometer, (P_i/P_i^o [-]), the amount of species **i** that is not retained during a given time t (~3 hours in the example) is given by Eq. A.1

$$\frac{\text{mol i not retained}}{\text{kg ZA}} = A_{ads,i}(t)\frac{P_i^o}{P_T}\frac{(\phi_v/60)}{22.4}\frac{10^3}{(m_{ZA}-\Delta m_{ZA})} \quad [\text{mol kg}^{-1}] \quad \text{(Eq. A.1)}$$

where $\mathbf{A_{ads,i}}$ [s^{-1}] corresponds to the area drawn by the normalized adsorption breakthrough curve until time t, ϕ_v [NmL min^{-1}] is the total volumetric flow of the feeding stream, $\mathbf{P_T}$ is the total pressure [kPa], $\mathbf{m_{ZA}}$ [mg] is the weight of zeolite A loaded to the bed, and $\mathbf{\Delta m_{ZA}}$ [mg] is the decrease in weight of the zeolite sample due to outgassing (16-18% m_{ZA}).

2. Calculation of the amount of species **i** fed to the reactor during the period t. This value can be obtained in an analogous way but considering the blank experimental breakthrough curve obtained at the same conditions:

$$\frac{\text{mol i fed}}{\text{kg ZA}} = A_{bl,i}(t)\frac{P_i^o}{P_T}\frac{(\phi_v/60)}{22.4}\frac{10^3}{(m_{ZA}-\Delta m_{ZA})} \quad [\text{mol kg}^{-1}] \qquad \text{(Eq. A.2)}$$

where $\mathbf{A_{bl,i}}$ [s^{-1}] corresponds to the area drawn by the normalized blank breakthrough curve until time t.

3. Calculation of the molar loading of species **i**, that is, the amount retained per kg of zeolite A.

$$q_i(t) = \left(\frac{\text{mol i fed}}{\text{kg ZA}} - \frac{\text{mol i not retained}}{\text{kg ZA}} \right) \qquad \text{(Eq. A.3)}$$

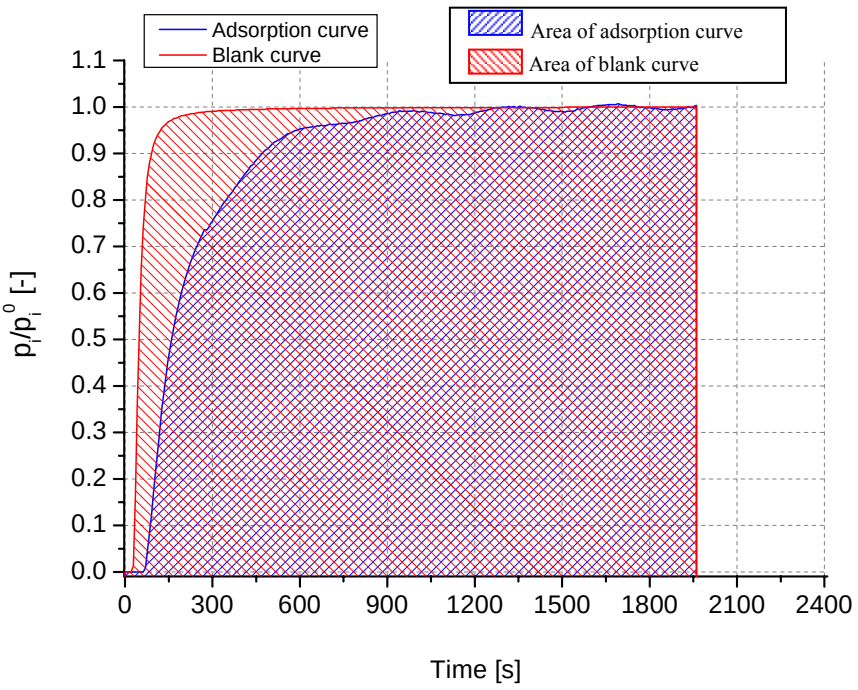

Figure A.1. Blank and adsorption normalized breakthrough curves obtained at 1460 Pa H_2O, 393 K during ~3 hours.

Substituting Eqs. A.1-A.2 in Eq. A.3 and rearranging yields Eq. A.4:

$$q_i(t) = \left[A_{bl,i}(t) - A_{ads,i}(t) \right] \frac{P_i^{in}}{P_T} \frac{(\phi_v / 60)}{22.4} \frac{10^3}{(m_{ZA} - \Delta m_{ZA})} \qquad \text{(Eq. A.4)}$$

For the experiment shown in Figure A.1, the equilibrium molar loading of water, q_w ($t \rightarrow \infty$) was:

$A_{bl,w} = 1899.1\ s$

$A_{ads,w} = 1724.4\ s$

$P_w^{in} = 1460\ Pa$

$\phi_V = 200.2\ cm^3\ (STP)\ min^{-1}$

$m_{ZA} = 103.2\ mg$

$\Delta m_{ZA} = 0.17\ m_{ZA}$

$\xrightarrow{(Eq\ A.5)}$ **$q_w\ (t \to \infty)$ =8.18 x 10^{-2} mol H_2O / kg ZA**

APPENDIX B

PROGRAM TO SIMULATE A ZEOLITE MEMBRANE REACTOR

The aim of the program is to simulate a tubular PV zeolite NaA membrane reactor to carry out the liquid-phase etherification reaction of 1-pentanol to DNPE catalyzed by a sulfonated resin. Before the simulation, the set of equations to model the PV membrane reactor (Eqs. V.3 and V.4 and boundary conditions) have been modified by substituting the axial coordinate **z** [m] by the corresponding dimensionless variable η defined as:

$$\eta = \frac{z}{L_b} \quad [-] \qquad \text{(Eq. B1)}$$

The resulting equation for the microscopic mass balance is given by Eqs. B2 and B3

$$\frac{\partial w_i^R}{\partial \eta} = \frac{\partial \left(w^R x_i \right)}{\partial \eta} = \left[\rho_S \left(1 - \varepsilon_b \right) r_i - N_i \, a_m \right] L_b A_b \ [\text{kmol h}^{-1}] \qquad \text{(Eq. B2)}$$

$$\frac{\partial w_i^P}{\partial \eta} = \frac{\partial \left(w^P y_i \right)}{\partial \eta} = -N_i \, a_m \, L_b \, A_b \ [\text{kmol h}^{-1}], \qquad \text{(Eq. B3)}$$

where w_i^R and w_i^P are molar flows of species **i**, respectively, at the retentate and permeate sides of the membrane tubes. The set of Eqs. B2 and B3 have been numerically solved through the finite element method as it is explained below. The position coordinates have been discretized by approximating the derivatives

$$\left(\partial w_i^R \big/ \partial \eta \right)_k \quad \text{and} \quad \left(\partial w_i^P \big/ \partial \eta \right)_k$$

to

$$\left(\frac{\partial w_i^R}{\partial \eta} \right)_k = \frac{w_i^{R,k} - w_i^{R,k-1}}{\Delta \eta} \quad \text{and} \quad \left(\frac{\partial w_i^P}{\partial \eta} \right)_k = \frac{w_i^{P,k} - w_i^{P,k-1}}{\Delta \eta} \qquad \text{(Eqs. B4 and B5)}$$

where k: axial position index (k = 1,…,m) and $\Delta\eta$ = 1/m. Eqs. B2 and B3 can be thus rewritten as Eqs. B6 and B7, respectively

$$w_i^{R,k} = w_i^{R,k-1} + \left[\rho_S \left(1 - \varepsilon_b \right) r_i^k - N_i \, a_m \right] L_b A_b \, \Delta \eta \qquad \text{(Eq. B6)}$$

$$w_i^{P,k} = w_i^{P,k-1} \left[\rho_S \left(1 - \varepsilon_b \right) r_i^k - N_i \, a_m \right] L_b A_b \, \Delta \eta, \qquad \text{(Eq. B7)}$$

where the molar fractions for axial position k at the retentate and permeate sides of the membranes can be calculated, respectively, by Eqs. B8 and B9

$$x_i^{R,k} = \frac{w_i^{R,k}}{\sum_{i=1}^{N} w_i^{R,k}} \quad \text{and} \quad x_i^{P,k} = \frac{w_i^{P,k}}{\sum_{i=1}^{N} w_i^{P,k}} \qquad \text{(Eqs. B.8 and B.9)}$$

It should be noted that the sign of $\mathbf{r_i^k}$ is (-) for reactants (1-pentanol) and (+) for products (water, DNPE, pentenes and other ethers). Finally, the related boundary conditions and the pressure drop through the bed (lumen of the tubes), $\mathbf{\Delta P_k}$ [kPa], can be calculated as follows

$$\eta = 0 \ (k=0) \ \rightarrow \ w_i^R = w_i^{R,o}, \ w_i^p = w_i^{P,o} = 0 \qquad \text{(Eq. B.10)}$$

$$\Delta P_k = P_o - P_k = (P_o - P_m) k \, \Delta\eta \qquad \text{(Eq. B.11)}$$

Equations B6-B10 are solved to calculate each **k** point. The molar fractions profiles are calculated slab-wise, that is, the value of axial position **k** is varied from 1 to m. At each position **k**, the composition of each species **i** is calculated iteratively according to the scheme shown in Figure B.1.

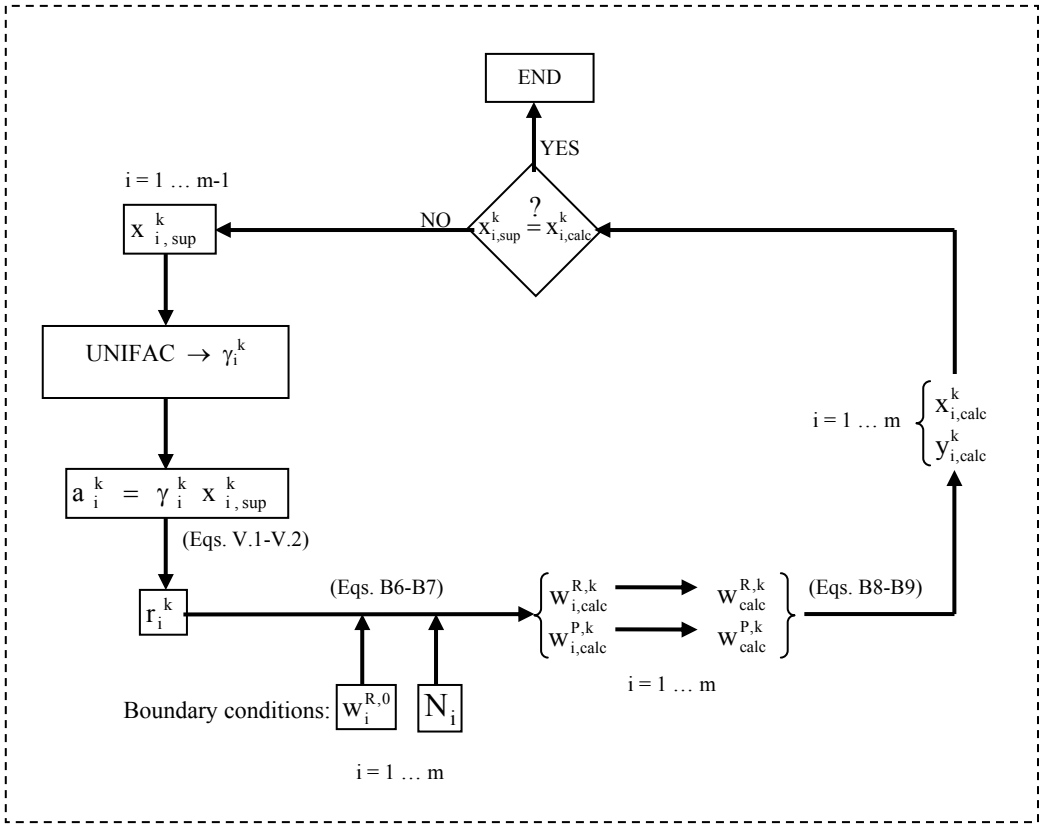

Figure B.1: Schematic representation of the procedure to simulate each finite position k of the PV zeolite membrane reactor. For the simulation of a fixed-bed reactor, N_i=0.

APPENDIX C

DETERMINATION OF ACTIVITY COEFFICIENTS OF A MIXTURE OF ADSORBED SPECIES

Like for vapor-liquid equilibrium (VLE), ideal solution behavior is seldom, because of the interactions between the adsorbed molecules and the adsorbed molecules with the solidsurface. To predict non-ideal mixture adsorption equilibria following the set of Eqs. VII.24, adsorbate activity coefficients, $\boldsymbol{\gamma_i(\Phi)}$ [-], have to be taken into account. As usual, the activity coefficient of the species **i** must approach unity for $x_i \rightarrow 1$ the infinite dilution value, $\boldsymbol{\gamma_i^{\infty}(\Phi)}$, as the composition of this species approaches zero for $x_i \rightarrow 0$.

The behavior for a mixture can be predicted if the coefficient $\boldsymbol{\gamma_i^{\infty}(\Phi)}$ is known. In fact, according to *Sakuth et al. (1998)*, the coefficient $\gamma_i^{\infty}(\Phi)$ can be experimentally determined from unary adsorption isotherm data only. Such a procedure involves two simplifications:

1. The adsorbate mole fractions of species 1 and 2 at $x_1 \rightarrow 0$ and $x_2 \rightarrow 0$ can be calculated, respectively, by using Eqs. C.1 and C.2

$$\lim_{x1 \to 1} x_1 = \frac{q_1(\Phi)}{q_2(\Phi)} \qquad \text{(Eq. C.1)}$$

$$\lim_{x2 \to 0} x_2 = \frac{q_2(\Phi)}{q_1(\Phi)}, \qquad \text{(Eq. C.2)}$$

   where the desired loadings of species 2 and 1 at the limitations $x_1 \rightarrow 0$ and $x_2 \rightarrow 0$ are realized in the case of the adsorption isotherm for the pure species.

2. The values of q_1 (at $x_1 \rightarrow 0$) and q_2 (at $x_2 \rightarrow 0$) can be approximated, respectively, by the Henry coefficient, He_i [mol kg^{-1} kPa^{-1}], of the pure species:

$$He_i = \lim_{P_i \to 0} \left[\frac{q_i(\Phi)}{P_i} \right]_T \qquad \text{(Eq. C.3)}$$

Taking into account both simplifications, the dilution activity coefficients of species 1 and 2, $\gamma_1^{\infty}(\Phi)$ and $\gamma_2^{\infty}(\Phi)$, can be obtained, respectively, by Eqs. C.4

$$\gamma_1^{\infty}(\Phi) = \frac{q_2(\Phi)}{He_1 \, P_1^{o}(\Phi)} \quad \text{and} \quad \gamma_2^{\infty}(\Phi) = \frac{q_1(\Phi)}{He_2 \, P_2^{o}(\Phi)} \qquad \text{(Eqs. C.4)}$$

For the special case that the unary adsorption of each species can be described by the single-site Langmuir isotherm, Eqs. C.4 are transformed into Eqs. C.5

$$\gamma_1^{\infty}(\Phi)=\frac{K_1 P}{(1+K_1 P)\ Ln(1+K_1 P)} \quad \text{and} \quad \gamma_2^{\infty}(\Phi)=\frac{K_2 P}{(1+K_2 P)\ Ln(1+K_2 P)} \qquad \text{(Eqs. C.5)}$$

As can be seen, the dilution activity coefficients of species 1 and 2 depend on the pressure of the gas or vapor phase and on the corresponding adsorption constant, but do not depend on saturation loadings.

On the other hand, using suitable g_E -models for the activity coefficient, the binary interaction parameters of the model can be calculated. In this work, the two-parameter Van Laar model (*Reid et al., 1987*), widely used to predict the non-ideal behavior of binary mixtures, is chosen for simplicity. According to this model, the activity coefficients of species 1 and 2 can be estimated by Eqs. C.6

$$RTLn[\gamma_1(\Phi)]=A_{12}\left(1+\frac{A_{12}}{A_{21}}\frac{x_1}{x_2}\right) \quad \text{and} \quad RTLn[\gamma_2(\Phi)]=A_{21}\left(1+\frac{A_{21}}{A_{12}}\frac{x_2}{x_1}\right), \quad \text{(Eq. C.6)}$$

where parameters A_{12} and A_{21} can be estimated from dilution activity coefficients by Eqs. C.7

$$A_{12}=RTLn\left[\gamma_1^{\infty}(\Phi)\right] \quad \text{and} \quad A_{21}=RTLn\left[\gamma_2^{\infty}(\Phi)\right], \qquad \text{(Eq. C.7)}$$

It should be stressed that the calculated activity coefficients of both species in the adsorbate with the Van Laar model are different from the values that can be obtained in the calculation of the VLE because of the effect of the surface potential of the solid surface, which is reflected in the values of the dilution activity coefficients. Moreover, these coefficients are always ≤1, which imply negative deviations from the Raoult's Law.

Figures C.1 and C.2 show the simulation trends of the activity coefficients in the adsorbate of species 1 (K_1 = 7.50 kPa) and 2 (K_2 = 0.75 kPa), that is K_1 : K_2 = 10 : 1, in a binary mixture with the composition of the former at a given vapor pressure and with the vapor pressure for a given composition, respectively. As can be seen in Figure VII.7, the activity coefficient of each species tends to increase with its molar composition from its dilution value to 1. Furthermore, Figure C.2 shows a decrease of the activity coefficients of both species with the vapor pressure, since the dilution activity coefficients of both species decrease with pressure by Eqs. C.5.

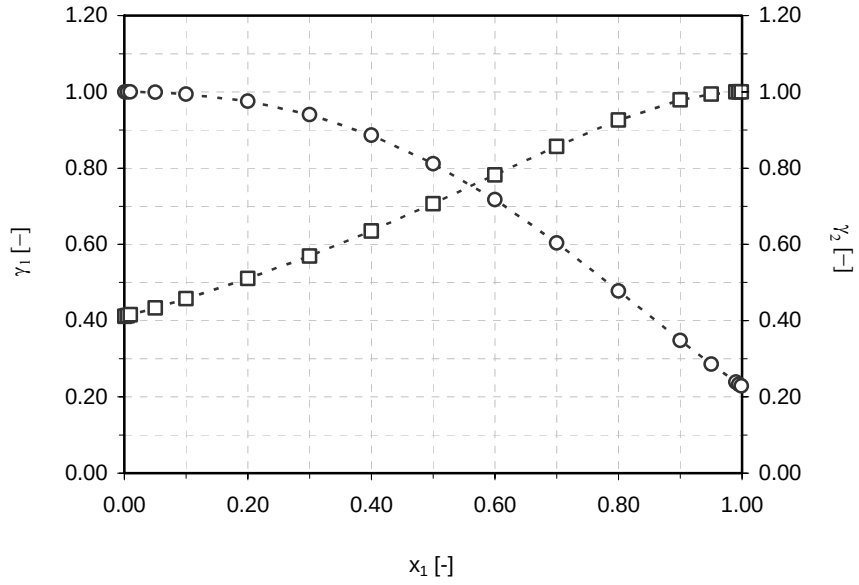

Figure C.1: Simulated trends of the activity coefficients of species 1 (squares) and 2 (cycles) in the adsorbate with the molar composition of species 1. Input data: $K_1 = 7.50$ kPa^{-1}, $K_2 = 0.75$ kPa^{-1}, T = 333 K, P = 10 kPa, $\gamma_1^{\infty}(\Phi) = 0.4107$, $\gamma_2^{\infty}(\Phi) = 0.2272$.

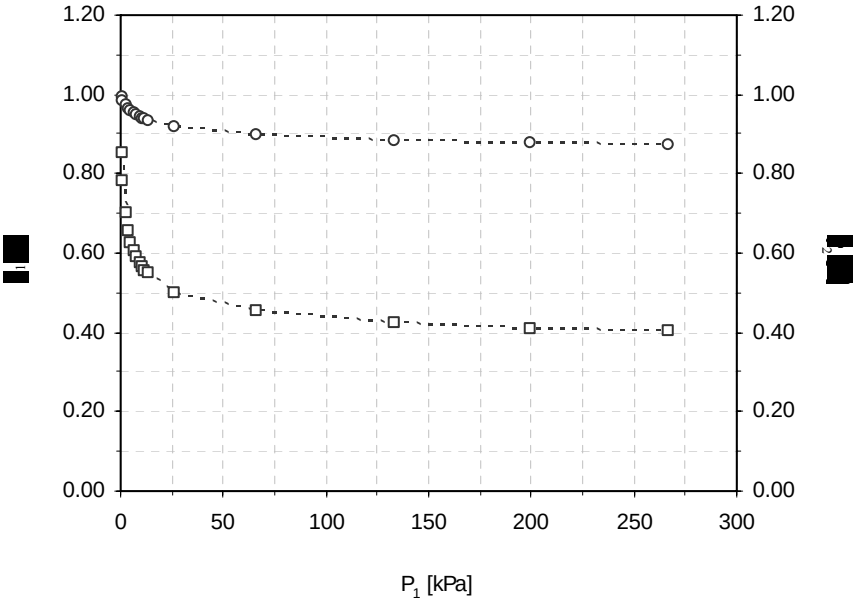

Figure C.2: Simulated trends of the activity coefficients of species 1 (squares) and 2 (cycles) in the adsorbate with the vapor pressure. Input data: $K_1 = 7.50$ kPa^{-1}, $K_2 = 0.75$ kPa^{-1}, T = 333 K, $x_1 = 0.30$.

APPENDIX D

FITTINGS OF N_2 ADSORPTION ISOTHERMS AT 77K TO THE TPI

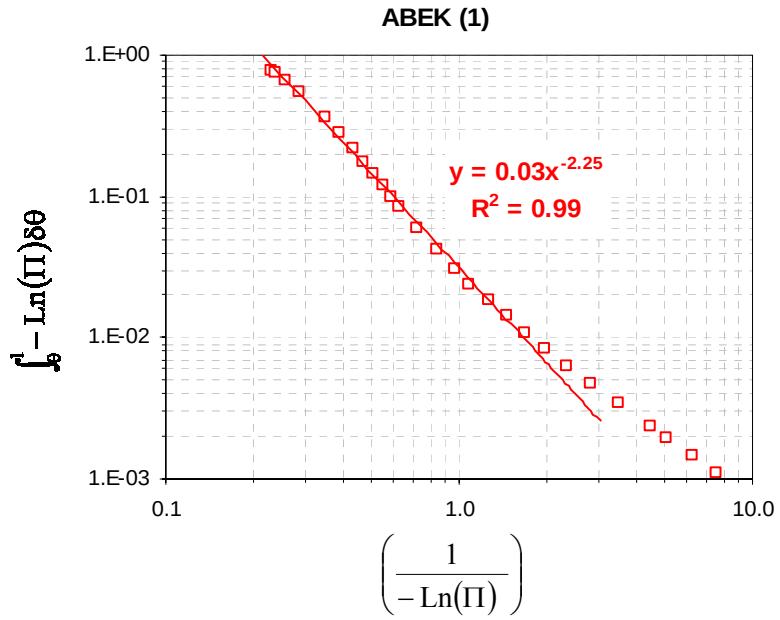

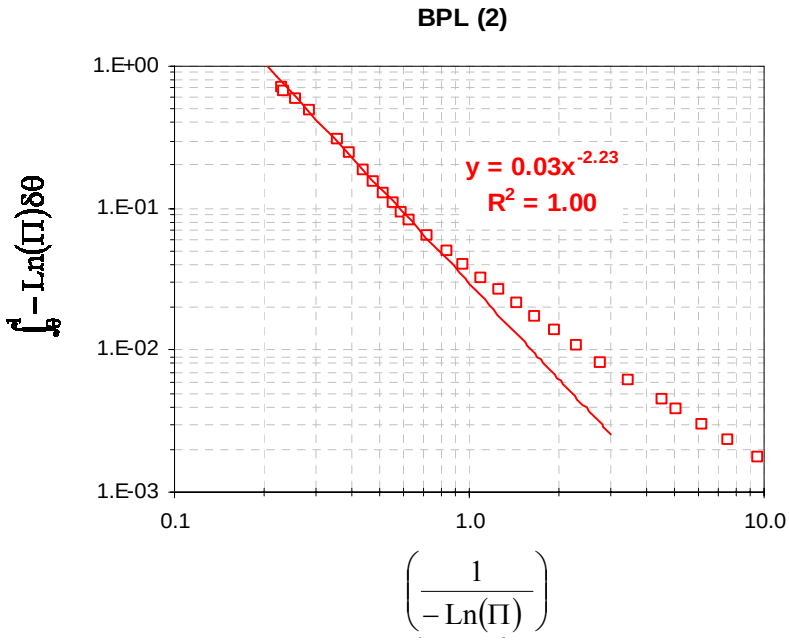

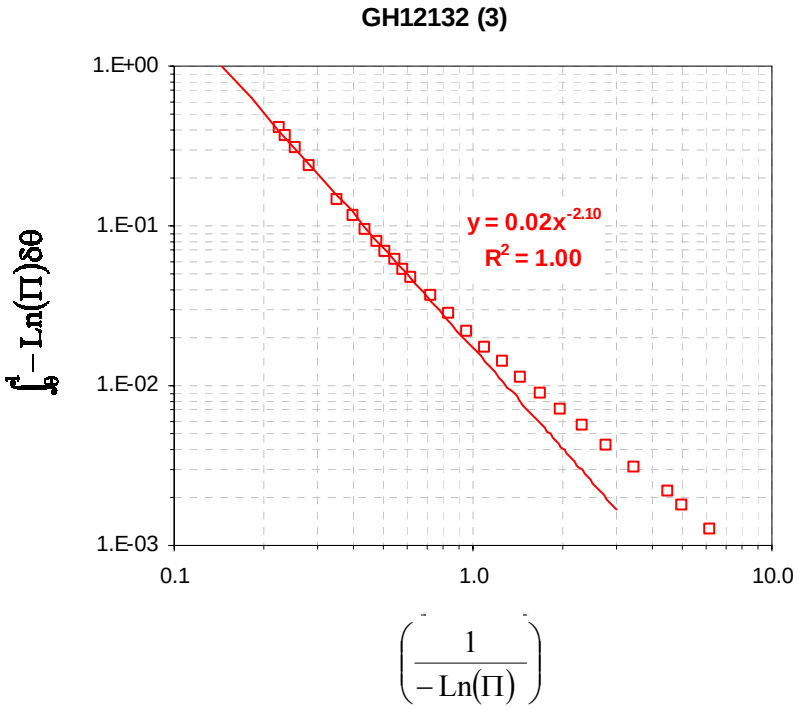
GH12132 (3)
1.E+00
1.E-01
1.E-02
1.E-03
0.1
1.0
10.0
y = 0.02x-2.10
R2 = 1.00
$\int_0^t -\mathrm{Ln}(\Pi)\delta\theta$
$\left(\frac{1}{-\mathrm{Ln}(\Pi)}\right)$

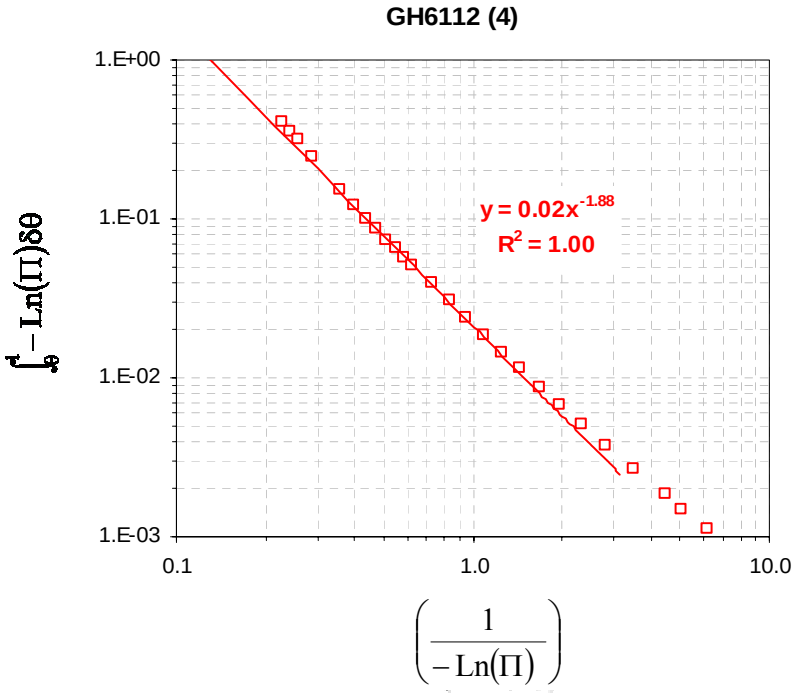
GH6112 (4)
1.E+00
1.E-01
1.E-02
1.E-03
0.1
1.0
10.0
y = 0.02x-1.88
R2 = 1.00
$\int_0^t -\mathrm{Ln}(\Pi)\delta\theta$
$\left(\frac{1}{-\mathrm{Ln}(\Pi)}\right)$

GMA (5)

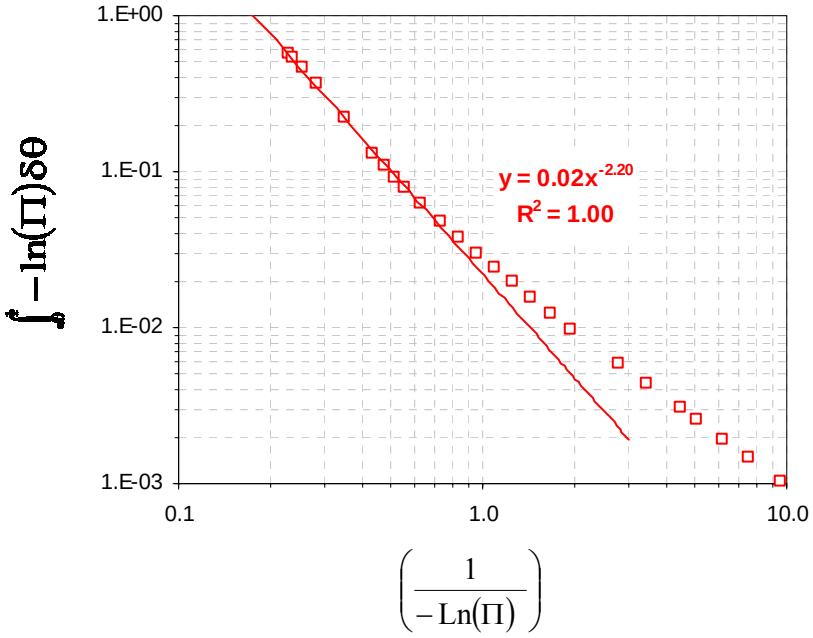
1.E+00
1.E-01
1.E-02
1.E-03
0.1
1.0
10.0
y = 0.02x-2.20
R2 = 1.00
$\int -\ln(\Pi)\delta\theta$
$\left(\frac{1}{-\mathrm{Ln}(\Pi)}\right)$

HRO (6)

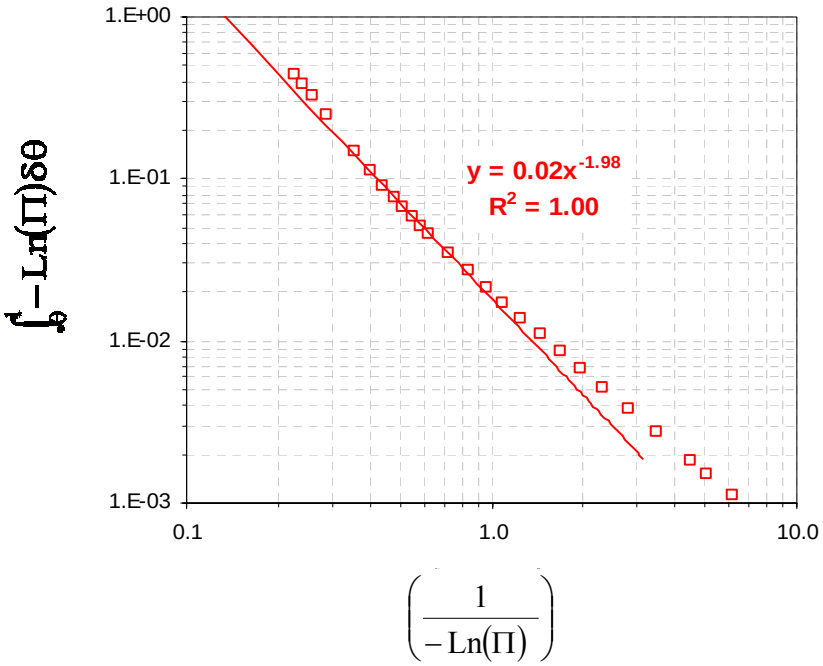
1.E+00
1.E-01
1.E-02
1.E-03
0.1
1.0
10.0
y = 0.02x-1.98
R2 = 1.00
$\int -\mathrm{Ln}(\Pi)\delta\theta$
$\left(\frac{1}{-\mathrm{Ln}(\Pi)}\right)$

PANRG (7)

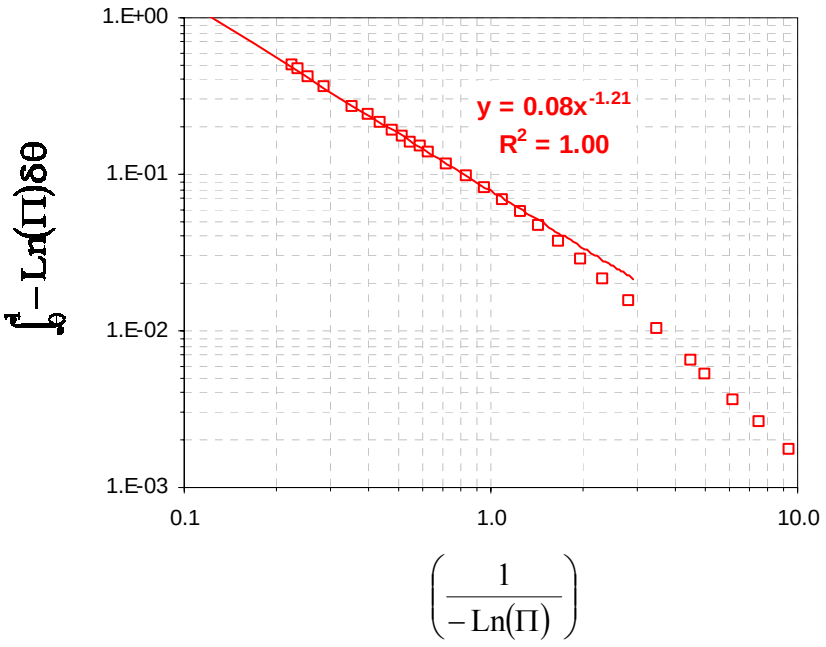

RBAA1 (8)

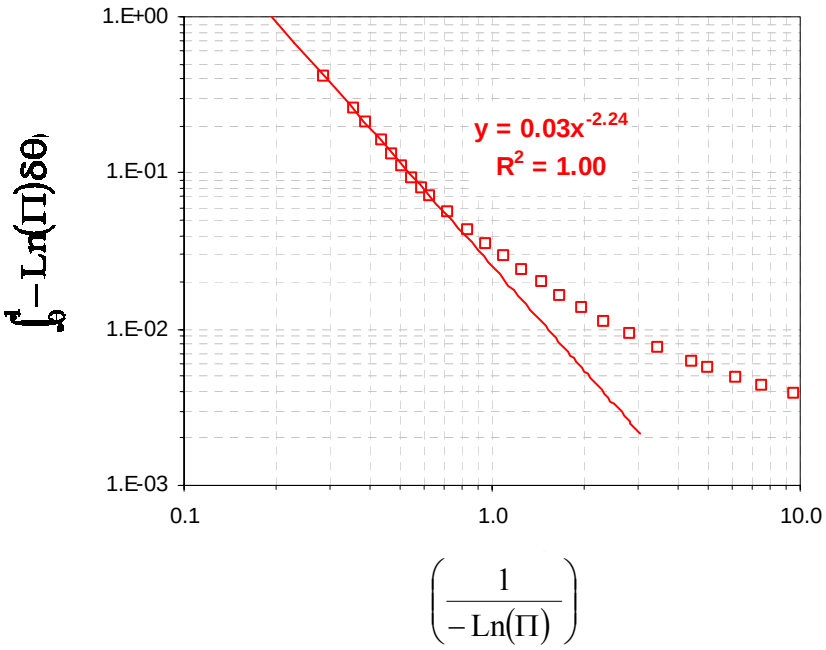

RGB (9)

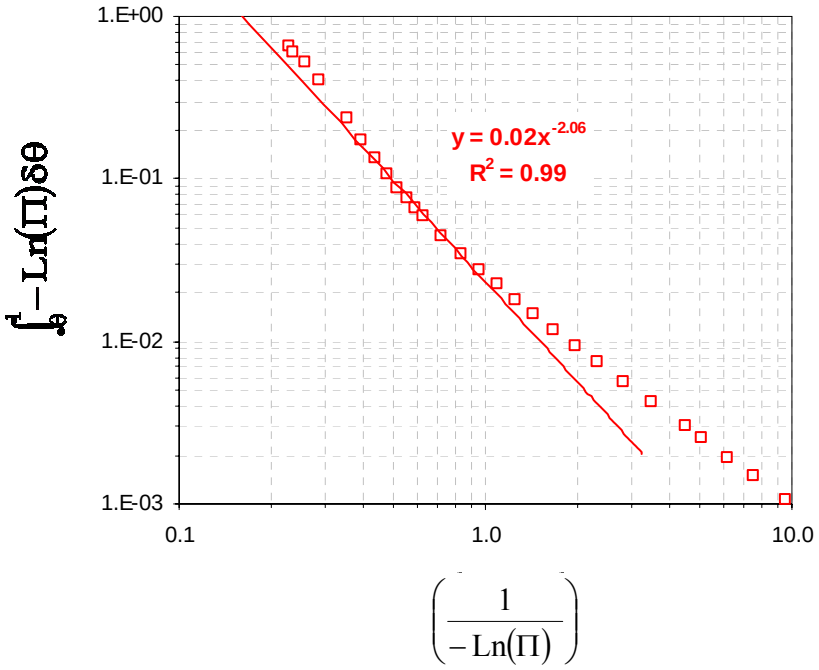

RGG08 (10)

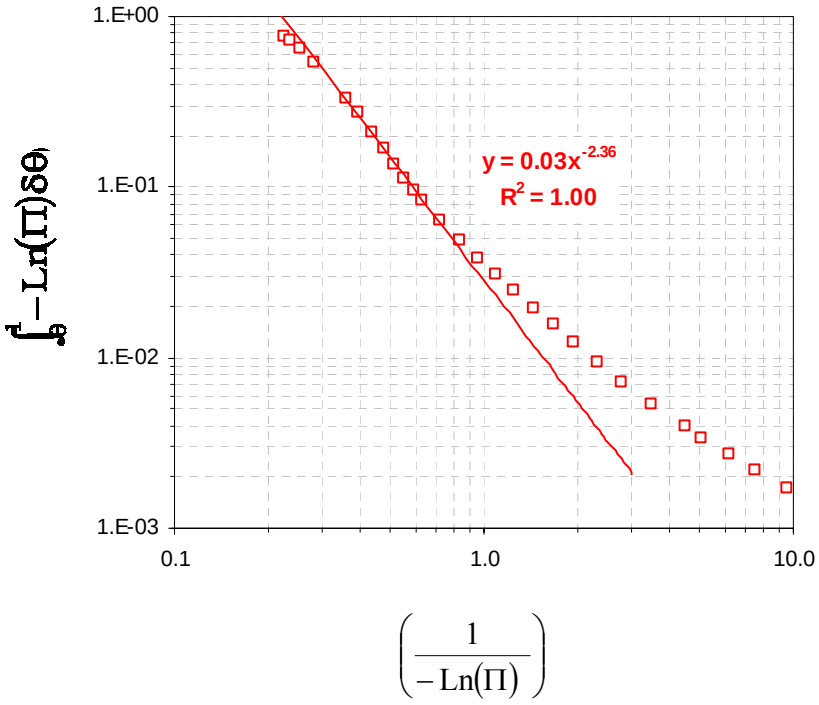

RGK (11)

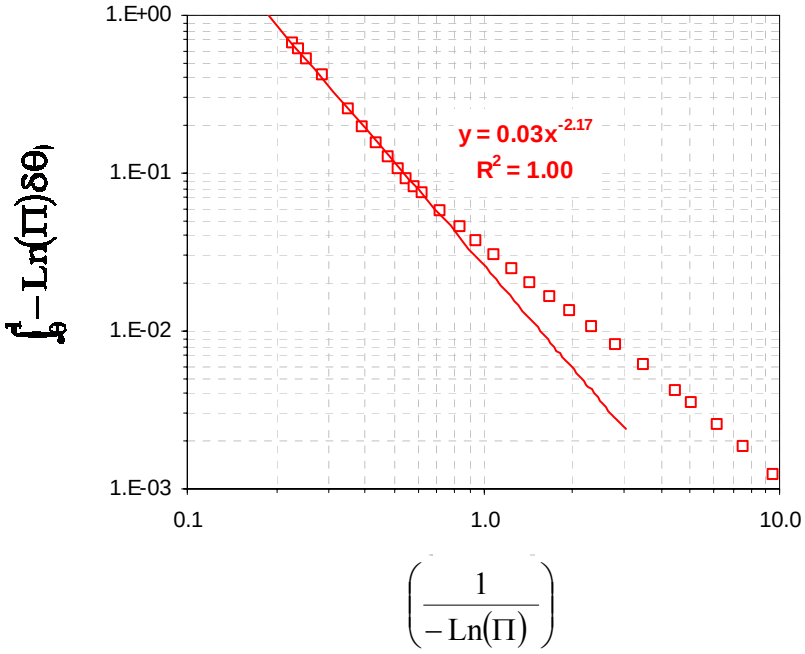

RZN1 (12)

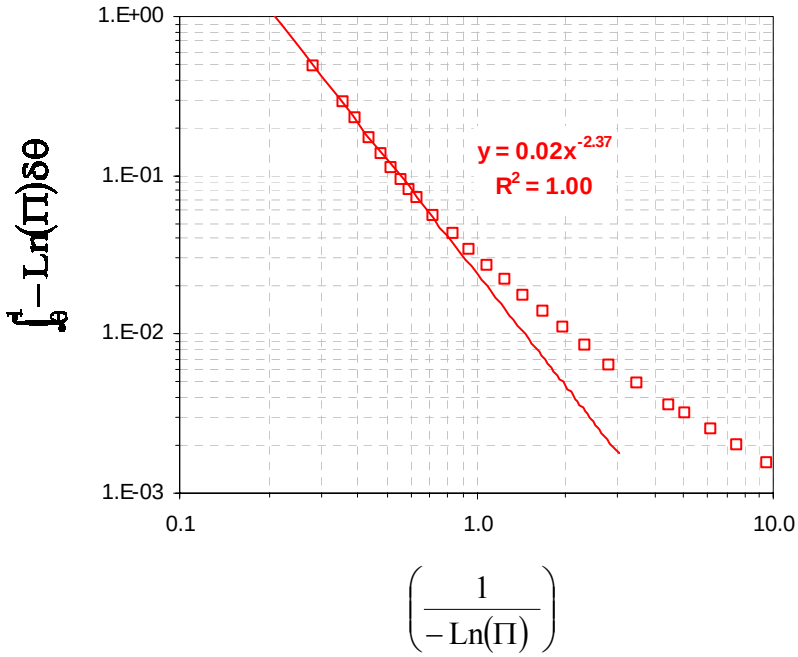

TA (13)

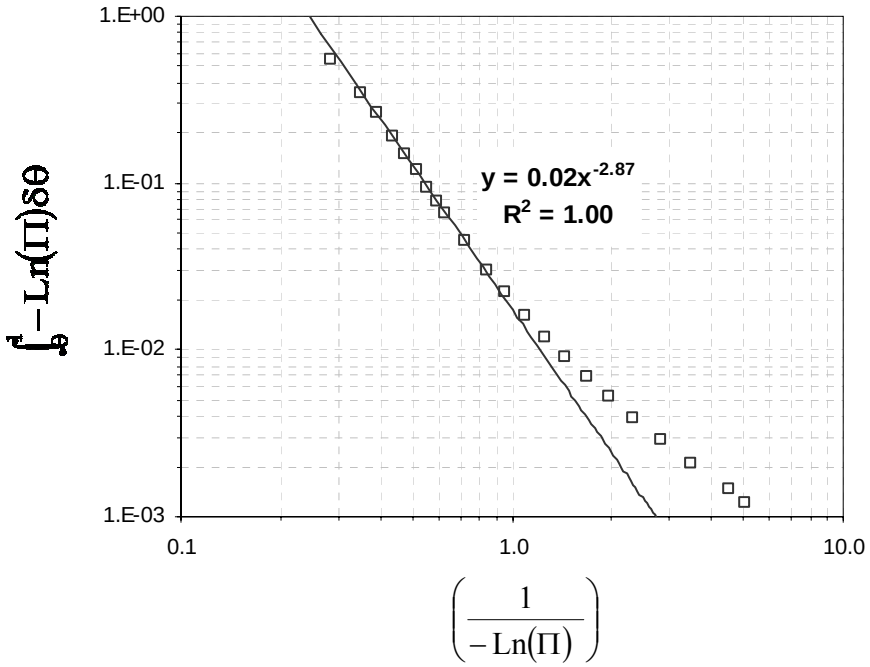

ZEOLITE A (14)

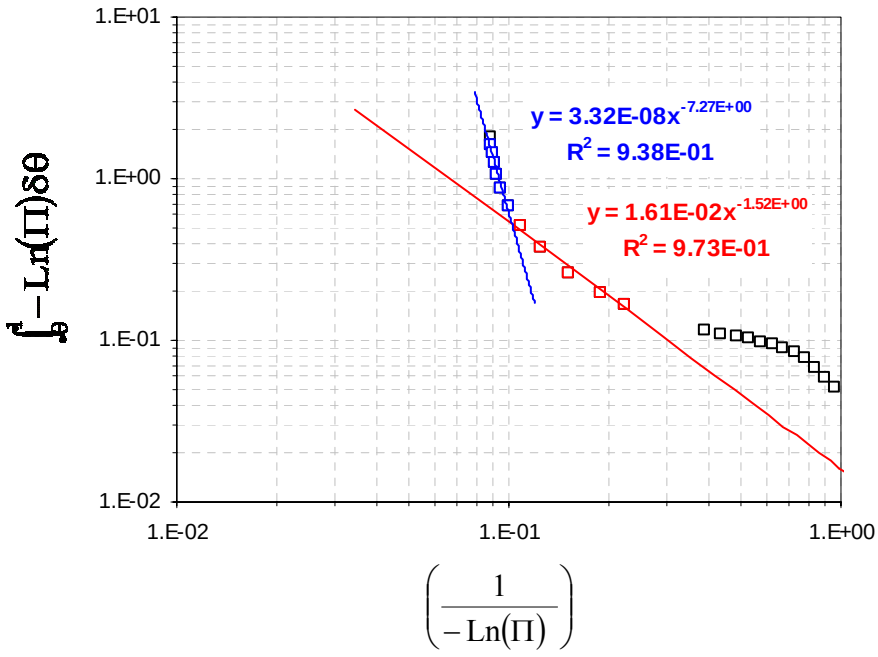

FAUJASITE (15)

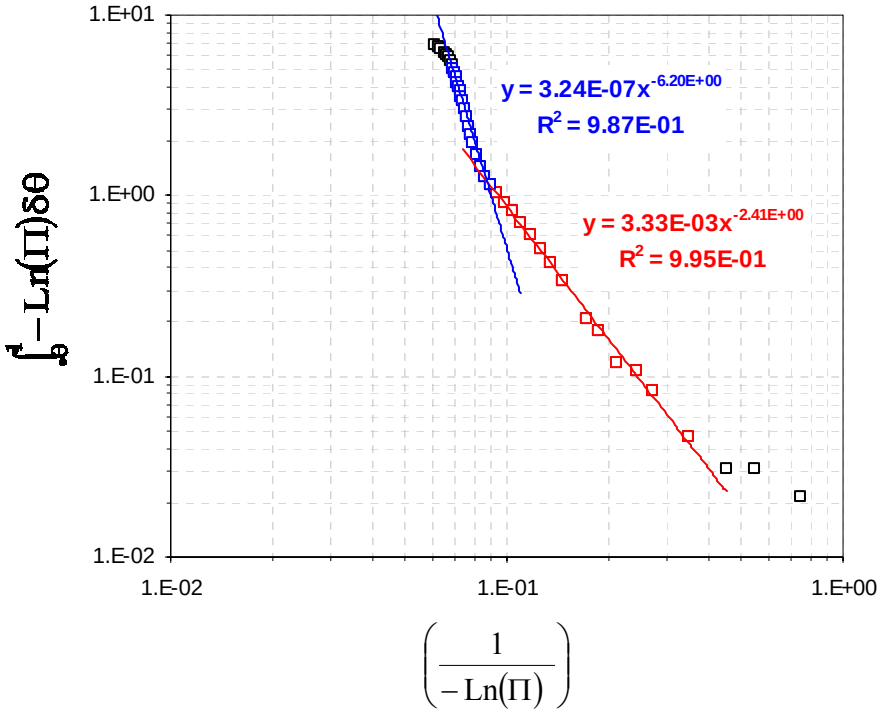

ZEOLITE X (16)

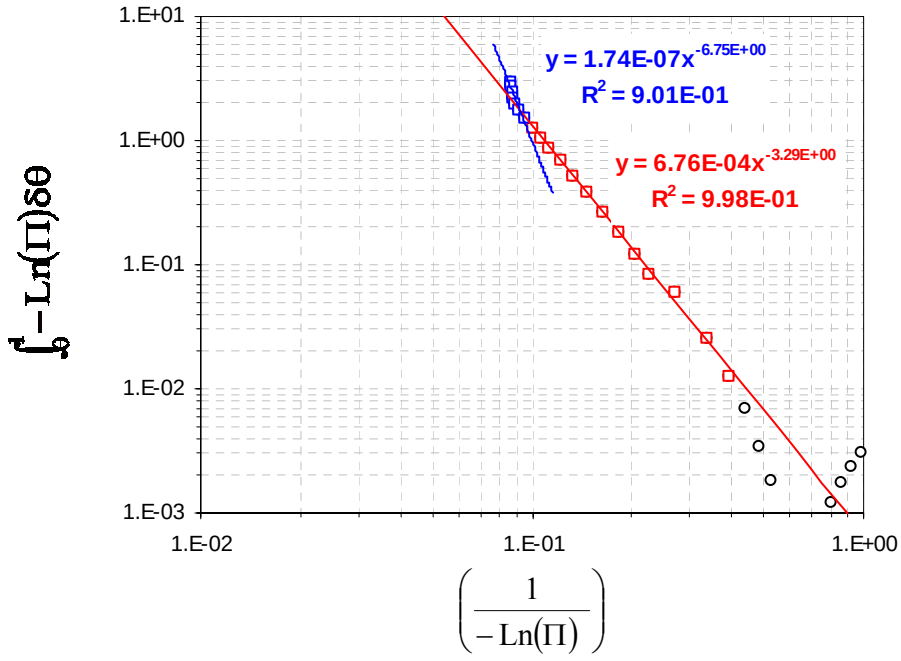

ZEOLITE β (17)

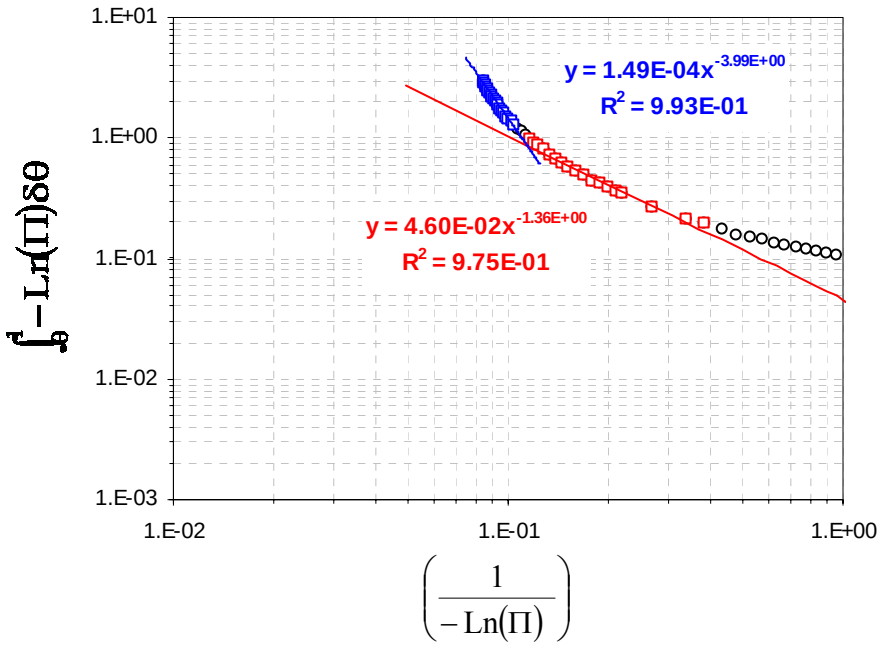

ZSM-5

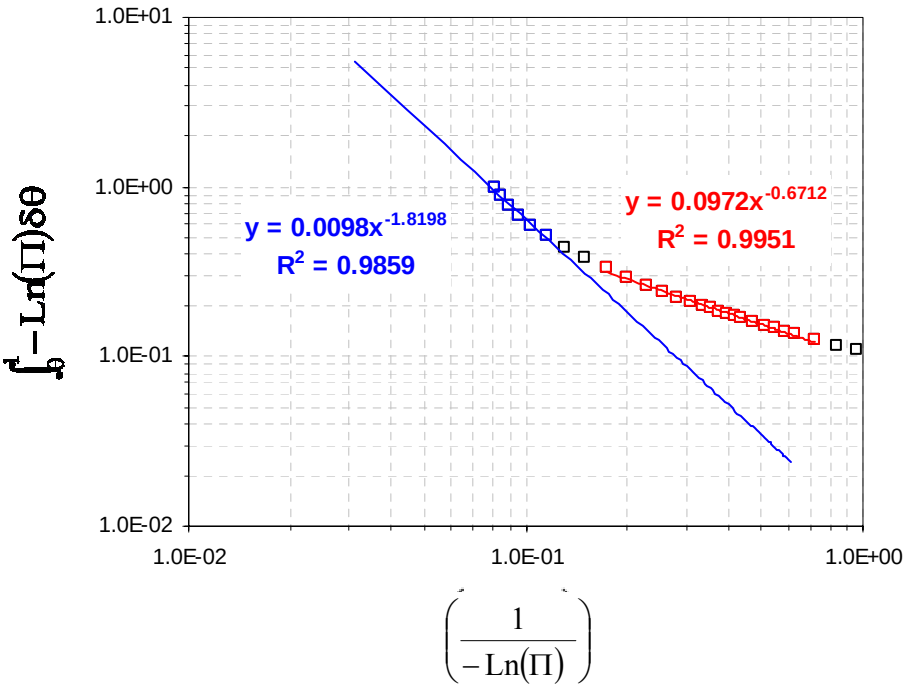

MORDENITE

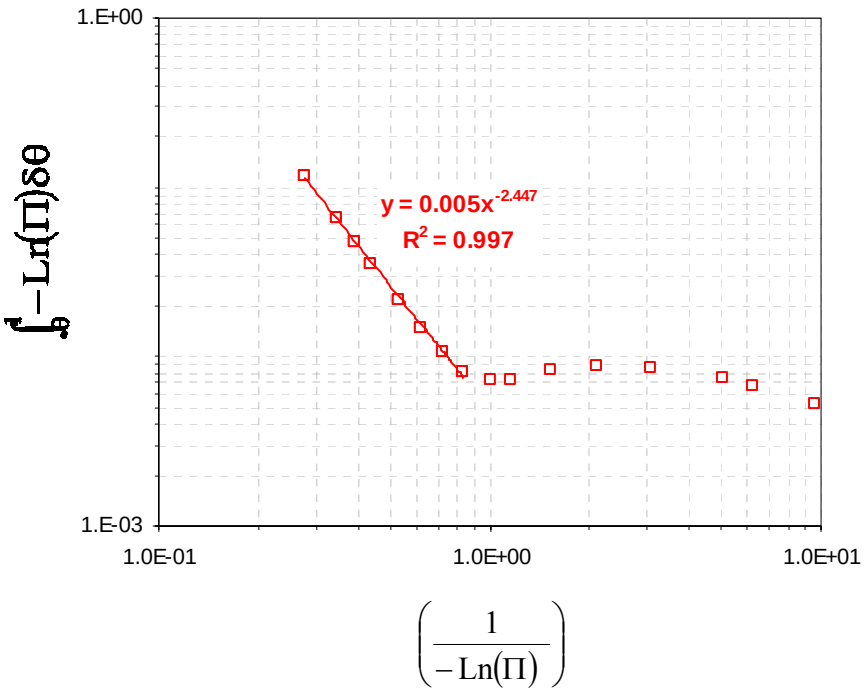
1.E+00
1.E-03
1.0E-01
1.0E+00
1.0E+01
y = 0.005x-2.447
R2 = 0.997
$\int_0^1 -\mathrm{Ln}(\Pi)\delta\theta$
$\left(\frac{1}{-\mathrm{Ln}(\Pi)}\right)$

APPENDIX E

ESTIMATION OF EXTERNAL MASS TRANSFER COEFFICIENTS (k_G)

E.1. Estimation of molecular diffusivities of water vapor ($D_{w\text{-}m}$)

The estimation of the molecular diffusivities of a dilute species **i** in a multicomponent gas mixture, $\mathbf{D_{i\text{-}m}}$ [$m^2\ s^{-1}$], can be reduced to the estimation of binary diffusivities, $\mathbf{D_{ij}}$, where **j** corresponds to the other species present in the mixture. For the special case of water vapor in the adsorption kinetics experiments described in chapter VIII, because its partial pressures are very low compared to that of the carrier gas (N_2) (0.1-3 kPa << ~101.3 kPa), the molecular diffusivity of water in the gas mixture can be approached by Eq. E.1 (*Reid et al.1987*):

$$D_{i-m} \approx D_{i-N_2} \qquad \text{(Eq. E.1)}$$

The binary diffusivities, D_{ij}, can be estimated by the Chapman- Enskog equation. For an ideal gas, this equation is reduced Eq. E.2 (*Levine, 1991*):

$$D_{ij} = \frac{0.00266\,T^{3/2}}{P\,\overline{M}^{1/2}\,\sigma_{ij}^2\,\Omega_D}, \qquad \text{(Eq. E.2)}$$

where σ_{ij} is the characteristic Lennard-Jones length [Å], Ω_D is the diffusion collision integral [-], and T and P are the temperature [K] and pressure [atm], respectively. Equation (E.2) is suitable for dilute gases at low pressures consisting of non-polar spherical molecules with molecular weight that do not differ significantly. However, because water is a polar molecule, Eq. E.2 is in principle inappropriate to estimate its molecular diffusivity. Brokaw suggested an alternative method, where Eq. E.2 is still used, but with a re-estimation of both where Ω_D and σ_{ij}. Firstly, Ω_D is estimated from a modification of the Neufield equation, which is given by Eq. E.3

$$\Omega_D = \frac{A}{(T^*)^B} + \frac{C}{\exp(D\,T^*)} + \frac{E}{\exp(F\,T^*)} + \frac{G}{\exp(H\,T^*)} + \frac{0.19\,\delta_{ij}^2}{T^*}, \qquad \text{(Eq. E.3)}$$

where A,…,H are constant parameters with values A=1.06036, B=0.15610 C=0.19300, D=0.47635, E=1.03587, F=1.52996, G=1.76474 and H=3.89411, and T^* is the so-called characteristic temperature given by Eq. E.4

$$T^* = \frac{k_B\,T}{\varepsilon_{ij}}, \qquad \text{(Eq. E.4)}$$

where ε_{ij} is the characteristic Lennard-Jones energy and k_B is the Boltzmann's constant. The parameters ε_{ij}, δ_{ij}, and σ_{ij} can be estimated, respectively, from the geometric mean of the pure parameter values ε_i, δ_i, and σ_i, respectively, defined by Eqs. E.5-E.7

$$\delta_i = \frac{1.94\cdot 10^3\,\mu_D^2}{V_b\,T_b}, \quad \frac{\varepsilon_i}{k_B} = 1.18\,(1+1.3\,\delta_i^2)\,T_{b_i}, \quad \sigma_i = \left(\frac{1.585\,\overline{V}_b}{1+1.3\,\delta_i^2}\right)^{1/3} \qquad \text{(Eqs. E.5-E.7)}$$

where μ_D, $\overline{V}_b$ and T_b are, respectively, the dipole moment, liquid molar volume at boiling point [$cm^3\ mol^{-1}$] and normal boiling point [K] of the pure species **i**. All these data are shown in the Table E.1. Furthermore, Table E.2 shows the calculated values for the $D_{w\text{-}N2}$ binary diffusivity for the temperature range 305-423 K.

Table E.1: Parameters of the pure species used to estimate $D_{w\text{-}N2}$ by the Brokaw's method

Parameter	N_2	H_2O
μ_D [D]*	0.0	1.8
V_b [$cm^3\ mol^{-1}$]**	31.2	18.9
T_b [K]*	77.35	373.15

* *Reid et al. (1996)*
** *Perry (1973)*

Table E.2: $D_{w\text{-}N2}$ diffusivities estimated by the Brokaw's method

T [K]	$D_{w\text{-}N2}\ x10^5\ [m^2\ s^{-1}]$
305	2.14
363	3.01
423	4.04

E.2. Determination of the EMT coefficients (k_G)

Different empirical correlations are available in the literature for fixed-bed reactors that can be used for the determination of $\mathbf{k_G}$ coefficients. These correlations are presented in terms of the dimensionless numbers of Sherwood (N_{Sh}), Schmidt (N_{Sc}), Re_p or $\overline{Re}$ and the "j" factor of Colburn ($\mathbf{j_D}$ [-]), which are defined, respectively, as follows:

$$N_{Sh} = \frac{k_G\,D_p}{D_{i-m}}, \quad N_{Sc} = \frac{\mu}{\rho\,D_{i-m}}, \quad \overline{Re} = \frac{Re_p}{(1-\varepsilon_b)}, \quad j_D = \frac{N_{Sh}}{Re_P\,N_{Sc}^{1/3}} \qquad \text{(Eqs. E.8-E.11)}$$

For the special case of low Re_p values (<0.01) and high bed porosities (>0.60), the Nelson and Galloway method is proposed (*Doraiswamy and Sharma, 1984*) to estimate k_g coefficients from Eqs. E.8-E.11

$$N_{Sh} = \frac{2\xi + \left\{ \frac{2\xi^2 (1-\varepsilon_b)^{1/3}}{\left[1-(1-\varepsilon_b)^{1/3}\right]^2} - 2 \right\} \tanh(\xi)}{\frac{\xi}{1-(1-\varepsilon_b)^{1/3}} - \tan(\xi)} \qquad 0.01 < Re_p < 1000 \qquad \text{(Eq. E.12)}$$

where $\xi = \left[\frac{1}{(1-\varepsilon_b)^{1/3}} - 1 \right] \frac{\alpha}{2} Re_p^{1/2} Sc^{1/3}$ with $\alpha \approx 0.6$

It should be noted that Eq. E.12 tends to Eqs. E.13 and E.14 for the following special cases:

1. $\boldsymbol{\varepsilon_b \to 1}$: A relationship similar to that presented for a single sphere by Frossling (1938) and Ranz (1952) (see *Doraiswamy and Sharma, 1984*) is obtained (Eq. E.13)

$$(N_{Sh})_{\varepsilon_b \to 0} = 2 + \alpha Re_p^{1/2} Sc^{1/3} \qquad \text{(Eq. E.13)}$$

2. $\boldsymbol{Re_p \to 0}$: The limiting value of the Sherwood number at $Re_p \to 0$ is described by Eq. E.14

$$(N_{Sh})_{Re_p \to 0} = \frac{1}{(1-\varepsilon_b)^{1/3}} \left[\frac{1}{(1-\varepsilon_b)^{1/3}} - 1 \right] \frac{\alpha^2}{2} Re_p Sc^{2/3} \qquad \text{(Eq. E.14)}$$

Table E.3 shows the estimated values of kg coefficients at the temperature range 305- 423 K.

Table E.3: EMT coefficients for water vapor, k_G, estimated by the three empirical correlations.

T [K]	N_{Sc} *[-]*	Re_p *[-]*	$\overline{Re}$ *[-]*	ξ *[-]*	N_{Sh} *[-]*	k_G *[cm s^{-1}]*
305	0.63	1.15E-02	2.87E-02	9.83E-03	7.58E-04	0.78
363	0.53	1.15E-02	2.87E-02	9.30E-03	6.78E-04	0.98
423	0.46	1.15E-02	2.87E-02	8.87E-03	6.16E-04	1.20

APPENDIX F

PROGRAM FOR THE DETERMINATION OF MS SURFACE DIFFUSIVITIES FROM UNARY ADSORPTION KINETICS

The aim of the program is to find the surface diffusivity of water and ethanol on zeolite A powder for both weak and strong confinements (see chapter VIII.1) from unary adsorption kinetic data obtained both in the microbalance and from breakthrough curve analysis in the differential packed bed equipped with mass spectroscopy analysis. The program also allows the statistical analysis of the fittings.

F.1. Determination of MS surface diffusivities at zero coverage

F.1.1. Profile of fractional loading in a spherical particle

Microscopic mass balance in spherical coordinates (Eq. F.1 or VIII.1)

$$\frac{\partial\theta}{\partial t}=\frac{1}{r^2}\frac{\partial}{\partial r}\left[r^2\,Đ(\theta)\frac{\partial\theta}{\partial r}\right], \qquad \text{(Eq. F.1)}$$

where θ is the fractional loading or surface coverage at each position of the particle ($0 \le \theta \le 1$) [-], **R** is the radius of the particle [m], r is the distance from the center of the particle ($0 \le r \le R$), **Đ** is the surface diffusivity of the species that is transferred from the outside to the inside of the particle [$m^2\ s^{-1}$], and t is the elapsed time [s]. Eq. F.1 is solved with the set of boundary and initial conditions (Eqs. F.2-F.4 or VIII.2-VIII.4) and through discretization using the Crank-Nicholson method.

Boundary conditions:

1) $\forall t,\ r = 0 \ \rightarrow\ \left.\frac{\partial\theta}{\partial t}\right|_{r=0} = 0$ (Eq. F.2)

2) $\forall t,\ r = R \ \rightarrow\ \theta = \theta_{eq}$ (Eq. F.3)

Initial conditions:

3) $t = 0,\ r \neq R \ \rightarrow\ \theta = 0$ (Eq. F.4)

$t = 0,\ r = R \ \rightarrow\ \theta = \theta_{eq}$

F.1.2. Discretization: Crank-Nicholson method

Equation: $\dfrac{\partial\theta}{\partial t} = \dfrac{1}{r^2}\dfrac{\partial}{\partial r}\left[r^2\, D(\theta)\dfrac{\partial\theta}{\partial r}\right]$

$\rho = \dfrac{r}{R} \longrightarrow \dfrac{\partial}{\partial r} = \dfrac{1}{R}\dfrac{\partial}{\partial \rho}$

$$\boxed{\frac{\partial\theta}{\partial t} = \frac{1}{R^2}\frac{\partial}{\partial\rho}\left[\rho^2\, D(\theta)\frac{\partial\theta}{\partial\rho}\right]}$$

t (i) ↓

$$\begin{array}{ccccc} & \vdots & \vdots & \vdots & \\ \cdots & \theta^{i}_{j-1} & \cdots\ \theta^{i}_{j} & \cdots\ \theta^{i}_{j+1} & \cdots \\ & \vdots & \vdots & \vdots & \\ \cdots & \theta^{i+1}_{j-1} & \cdots\ \theta^{i+1}_{j} & \cdots\ \theta^{i+1}_{j+1} & \cdots \\ & \vdots & \vdots & \vdots & \end{array}$$

$\longrightarrow$ ρ (j)

$$D^{i+1}_{j+\frac{1}{2}} = D\left(\frac{\theta^{i+1}_{j+1} + \theta^{i+1}_{j}}{2}\right) \approx D^{i}_{j+\frac{1}{2}} \qquad D^{i+1}_{j-\frac{1}{2}} = D\left(\frac{\theta^{i+1}_{j} + \theta^{i+1}_{j-1}}{2}\right) \approx D^{i}_{j-\frac{1}{2}}$$

$\rho_k = k\,\Delta\rho$

Discretization:

$$\frac{\theta^{i+1}_{j} - \theta^{i}_{j}}{\Delta t} = \frac{1}{2R^2\rho_j^2(\Delta\rho)^2}\left[\rho^2_{j+\frac{1}{2}} D^{i}_{j+\frac{1}{2}}\left(\theta^{i+1}_{j+1} - \theta^{i+1}_{j}\right) - \rho^2_{j-\frac{1}{2}} D^{i}_{j-\frac{1}{2}}\left(\theta^{i+1}_{j} - \theta^{i+1}_{-1j}\right) + \rho^2_{j+\frac{1}{2}} D^{i}_{j+\frac{1}{2}}\left(\theta^{i}_{j+1} - \theta^{i}_{j}\right) - \rho^2_{j-\frac{1}{2}} D^{i}_{j-\frac{1}{2}}\left(\theta^{i}_{j} - \theta^{i}_{j-1}\right)\right]$$

$$\frac{\theta_j^{i+1}-\theta_j^i}{\Delta t}=\frac{1}{2R^2\rho_j^2}\left[\left(j+\frac{1}{2}\right)^2 D^i_{j+\frac{1}{2}}\left(\theta_{j+1}^{i+1}-\theta_j^{i+1}\right)-\left(j-\frac{1}{2}\right)^2 D^i_{j-\frac{1}{2}}\left(\theta_j^{i+1}-\theta_{-1j}^{i+1}\right)+\left(j+\frac{1}{2}\right)^2 D^i_{j+\frac{1}{2}}\left(\theta_{j+1}^{i}-\theta_j^{i}\right)-\left(j-\frac{1}{2}\right)^2 D^i_{j-\frac{1}{2}}\left(\theta_j^{i}-\theta_{j-1}^{i}\right)\right]$$

$$\theta_j^{i+1}-\theta_j^i=\frac{\Delta t}{2R^2(\Delta\rho)^2}\left[\left(1+\frac{1}{2j}\right)^2 D^i_{j+\frac{1}{2}}\left(\theta_{j+1}^{i+1}-\theta_j^{i+1}+\theta_{j+1}^{i}-\theta_j^{i}\right)-\left(1-\frac{1}{2j}\right)^2 D^i_{j-\frac{1}{2}}\left(\theta_j^{i+1}-\theta_{-1j}^{i+1}+\theta_j^{i}-\theta_{j-1}^{i}\right)\right]$$

$$\frac{2R^2(\Delta\rho)^2}{\Delta t}\theta_j^{i+1}-D^i_{j+\frac{1}{2}}\left(\theta_{j+1}^{i+1}-\theta_j^{i+1}\right)+\left(1-\frac{1}{2j}\right)^2 D^i_{j-\frac{1}{2}}\left(\theta_j^{i+1}-\theta_{j-1}^{i+1}\right)=\frac{2R^2(\Delta\rho)^2}{\Delta t}\theta_j^{i}+D^i_{j+\frac{1}{2}}\left(\theta_{j+1}^{i}-\theta_j^{i}\right)-\left(1-\frac{1}{2j}\right)^2 D^i_{j-\frac{1}{2}}\left(\theta_j^{i}-\theta_{j-1}^{i}\right)$$

$$\frac{2R^2(\Delta\rho)^2}{\Delta t}\theta_j^{i+1}-\left(1+\frac{1}{2j}\right)^2 D^i_{j+\frac{1}{2}}\left(\theta_{j+1}^{i+1}-\theta_j^{i+1}\right)+\left(1-\frac{1}{2j}\right)^2 D^i_{j-\frac{1}{2}}\left(\theta_j^{i+1}-\theta_{j-1}^{i+1}\right)=$$

$$=\frac{2R^2(\Delta\rho)^2}{\Delta t}\theta_j^{i}+\left(1+\frac{1}{2j}\right)^2 D^i_{j+\frac{1}{2}}\left(\theta_{j+1}^{i}-\theta_j^{i}\right)-\left(1-\frac{1}{2j}\right)^2 D^i_{j-\frac{1}{2}}\left(\theta_j^{i}-\theta_{j-1}^{i}\right)$$

$$-\left(1-\frac{1}{2j}\right)^2 D^i_{j-\frac{1}{2}}\theta_{j-1}^{i+1}+\left[\frac{2R^2(\Delta\rho)^2}{\Delta t}+\left(1+\frac{1}{2j}\right)^2 D^i_{j+\frac{1}{2}}+\left(1-\frac{1}{2j}\right)^2 D^i_{j-\frac{1}{2}}\right]\theta_j^{i+1}-\left(1+\frac{1}{2j}\right)^2 D^i_{j+\frac{1}{2}}\theta_{j+1}^{i+1}=$$

$$=\left(1-\frac{1}{2j}\right)^2 D^i_{j-\frac{1}{2}}\theta_{j-1}^{i}+\left[\frac{2R^2(\Delta\rho)^2}{\Delta t}-\left(1+\frac{1}{2j}\right)^2 D^i_{j+\frac{1}{2}}-\left(1-\frac{1}{2j}\right)^2 D^i_{j-\frac{1}{2}}\right]\theta_j^{i}+\left(1+\frac{1}{2j}\right)^2 D^i_{j+\frac{1}{2}}\theta_{j+1}^{i}$$

Boundary condition 1: $\left.\frac{\partial\theta}{\partial r}\right|_{r=0} = 0 \equiv \theta_0 = \theta_1 \qquad (j=1)$

$$\left[\frac{2R^2(\Delta\rho)^2}{\Delta t}+\left(\frac{3}{2}\right)^2 D^i_{3/2}\right]\theta_1^{i+1}-\left(\frac{3}{2}\right)^2 D^i_{3/2}\,\theta_2^{i+1}=\left[\frac{2R^2(\Delta\rho)^2}{\Delta t}-\left(\frac{3}{2}\right)^2 D^i_{3/2}\right]\theta_1^i+\left(\frac{3}{2}\right)^2 D^i_{3/2}\,\theta_2^i$$

Boundary condition 2: $\theta^{i+1}(R)=\theta_{eq}^{i+1} \quad (j=m-1) \longrightarrow \theta_{j+1}^{i+1}=\theta_{eq}^{i+1}$

Initial condition: $\theta(t=0)=0 \qquad \forall j \neq m$

$$-\left(1-\frac{1}{2j}\right)^2 D^i_{j-\frac{1}{2}}\,\theta_{j-1}^{i+1}+\left[\frac{2R^2(\Delta\rho)^2}{\Delta t}+\left(1+\frac{1}{2j}\right)^2 D^i_{j+\frac{1}{2}}+\left(1-\frac{1}{2j}\right)^2 D^i_{j-\frac{1}{2}}\right]\theta_j^{i+1}-\left(1+\frac{1}{2j}\right)^2 D^i_{j+\frac{1}{2}}\,\theta_j^{i+1}=$$

$$=\left(1-\frac{1}{2j}\right)^2 D^i_{j-\frac{1}{2}}\,\theta_{j-1}^{i}+\left[\frac{2R^2(\Delta\rho)^2}{\Delta t}-\left(1+\frac{1}{2j}\right)^2 D^i_{j+\frac{1}{2}}-\left(1-\frac{1}{2j}\right)^2 D^i_{j-\frac{1}{2}}\right]\theta_j^{i}+\left(1+\frac{1}{2j}\right)^2 D^i_{j+\frac{1}{2}}\,\theta_{eq}^{i+1}$$

F.1.3. Mean fractional loading of a particle of radius R ($\bar{\theta}$)

$$\bar{\theta} = \frac{\int_V \theta \delta V}{\int_V \delta V} = \frac{\int_0^R \theta 4\pi r^2 \delta r}{\frac{4}{3}\pi R^3} = \frac{3}{R^3}\int_0^R \theta r^2 \delta r \qquad \text{(Eq. F.5)}$$

F.1.4. Mean fractional loading of a bed of particles of radius R_i ($\bar{\bar{\theta}}$)

$$\bar{\bar{\theta}} = \frac{\int_{-\infty}^{+\infty} \nu(R)\bar{\theta}\delta V}{\int_{-\infty}^{+\infty} \nu(R)\delta V} = \frac{\int_{-\infty}^{+\infty} \nu(R)\bar{\theta} 4\pi R^2 \delta R}{\int_{-\infty}^{+\infty} \nu(R) 4\pi R^2 \delta R} = \frac{\int_{-\infty}^{+\infty} \nu(R)\bar{\theta} R^2 \delta R}{\int_{-\infty}^{+\infty} \nu(R) R^2 \delta R} \qquad \text{(Eq. F.6)}$$

where R_i is the radius of a particle of radius **i** [m], ν_i and $\bar{\theta}_i$ are, respectively, the relative frequency [-] and the mean loading [-] of the particle of radius R_i according to Figure VII.2 and $\bar{\bar{\theta}}$ is the loading [-] of the bed of particles.

F.1.5. Optimization of parameter $Đ^S(0)$

Parameter $Đ^S(0)$ is optimized for each model diffusivity (see Eqs. VIII.7 and VIII.8) by minimizing the sum of squares of mean fractional loading of the bed by comparing experimental with predicted fractional loading data. The fractional loading is calculated slab-wise, that is, the value of axial position **j** is varied from 1 to m for each time **i** according to the scheme shown in Figure F.1. Moreover, Figure F.2 shows a scheme of the program used for carrying out the fittings of experimental data to the model.

F.2. Estimation of confidence intervals for fitted parameters for non-linear models (*Himmelblau, 1970*).

The individual confidence interval for each parameter δ_i of a nonlinear model for a significance level α can be estimated by the following equation:

$$\delta_i = d_i \pm t_{1-\alpha/2} S_{\bar{Y}_i} C_{ii}^{0.5}; \qquad \text{(Eq. F.7)}$$

where d_i is the estimated value of the parameter δ_i, t is the Student-t used in the t-test, $S^2_{\bar{Y}_i}$ is the estimated variance of $\bar{Y}_i$, which is the sample average of observed Y´s at x_i points, and C_{ii} is the value of the diagonal of the matrix C, given by:

$$C = \left(X^T \times X\right)^{-1} \qquad \text{(Eq. F.8)}$$

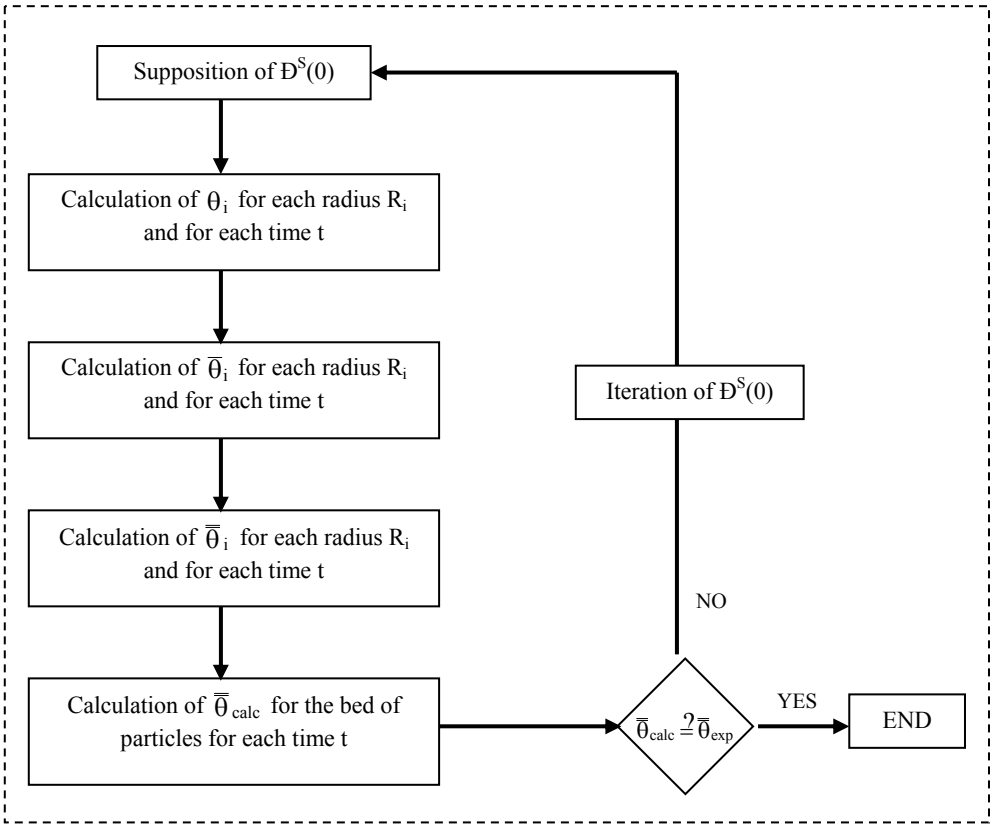

Figure F.1: Schematic representation of the procedure to fit $Đ^S(0)$ parameters for both water and ethanol adsorption on zeolite NaA powder.

where X is an $(n \times m)$ matrix defined as:

$$[X_{ij}] = \frac{\partial \eta_i(x_i)}{\partial \delta_j} \qquad \text{(Eq. F.11)}$$

with **i**: experimental point index i: 1,..., n
j: fitting parameter index j: 1,..., m

where $\eta_i(x_i)$ is the nonlinear model evaluated at the x_i point. The application of this method to determine the confidence intervals of the m=1 parameter of the model fitted to the adsorption kinetics of water and ethanol at 1-3 h leads to a (n x 1) matrix, where **n** is the number of experimental points of each curve. The function $\eta_i(x_i)$ corresponds to the fitted adsorption kinetic curve. An estimation of the partial derivates to obtain $[X_{ij}]$ has been performed by varying ±1% each d_i parameter while the rest are constant. These variations have been found satisfactory as the same results were obtained for variations in the range of

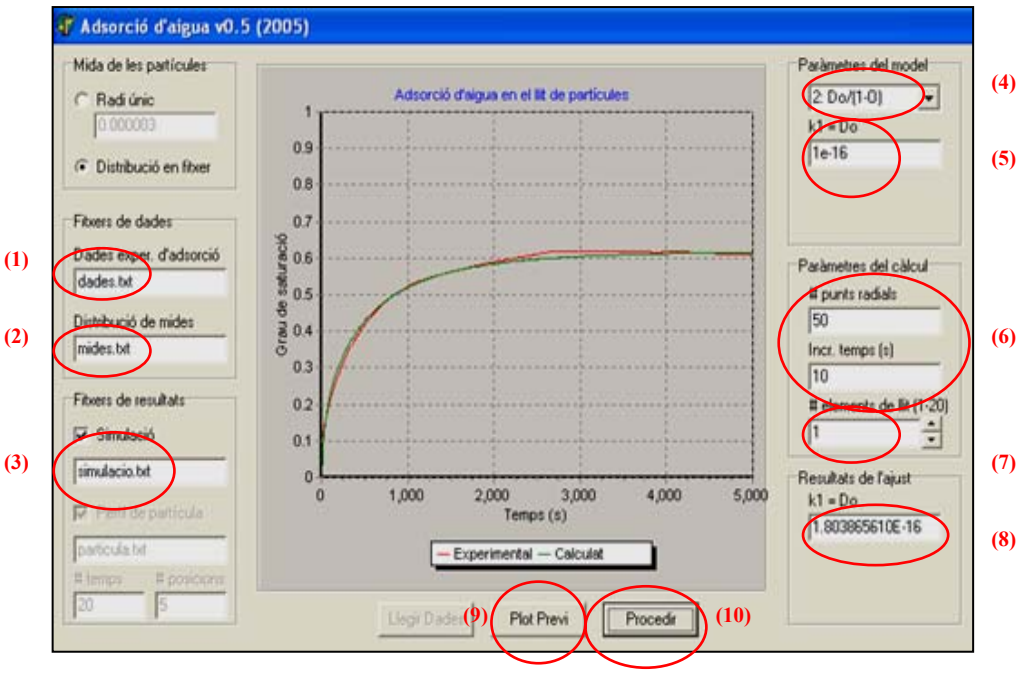

Figure E.2 Screen of the program used to optimize surface diffusivities. (1) Input file for experimental kinetic adsorption data, (2) Input file for particle size distribution, (3) Output file for fractional loading profile within the particle, (4) Surface diffusivity model, (5) Initial value for surface diffusivity at zero fractional loading, (6) Number of radial and time finite elements, (7) Number of finite elements of the packed bed, (8) Optimized surface diffusivity at zero fractional loading, (9) Previous plot of experimental data, (10) Fitting.

± 0.1-5% of each parameter d_i. The value of $t_{1-\alpha/2}$ was taken as 1.96, for an infinite number of degrees of freedom with a 95% confidence interval. The variance $S_{\overline{Y_i}}$ was estimated by the following expression:

$$S^2_{\overline{Y_i}} = S^2_r + S^2_e \qquad \text{(Eq. F.12)}$$

where S^2_r and S^2_e are, respectively, the residual and error mean squares, which are defined by the following equations:

$$S^2_r = \frac{\sum_{i=1}^{n} p_i (\overline{Y_i} - \hat{Y}_i)^2}{n-2} = \frac{SQ}{n-2} \qquad S^2_e = \frac{\sum_{i=1}^{n} \sum_{j=1}^{p_i} (Y_{i,j} - \overline{Y}_i)^2}{\sum_{i=1}^{n} p_i - n} \qquad \text{(Eqs. F.13 and F.14)}$$

where $Y_{i,j}$ is the j^{th} observation of Y at x_i, $\hat{Y}_i$ is the estimated value at x_i, $\mathbf{p_i}$ is the number of replicate measurements (in case that no replicate values are available, p_i takes the value 1) and **n** is the number of data points.

APPENDIX G

PROGRAM FOR THE DETERMINATION OF ALPHA COEFFICIENTS IN EQS. VIII.66 AND VIII.67

The aim of the program is find the alpha coefficients in Eqs. VIII.66 and VIII.67 that allow the determination of surface diffusivities of water and ethanol from steady-state PV data obtained in zeolite NaA membranes.

Partial pressure profile of species i across a zeolite NaA layer

Microscopic mass balance for species **i** in Cartesian coordinates:

$$\frac{\delta P_i}{\delta \eta} = -\alpha_i \frac{q_{M,i}}{q_i\, f(q_T)} P_i, \qquad \text{(Eq. G.1)}$$

where P_i is the partial pressure [kPa], $\eta = z/\ell_{ZA}$ is the dimensionless position within the zeolite NaA layer thickness [-], q_i is the molar loading [mol kg^{-1}], $f(q_T)$ the function of the total loading related to surface diffusivity, and α_i the alpha-parameter to be optimized. Eq. G.1 can be numerically solved as it is explained below. The coordinates have been discretized by approximating the derivative in Eq. G.1 to finite differences as it is explained below

$$\frac{\delta P_i}{\delta \eta} = \frac{P_i^k - P_i^{k-1}}{\Delta \eta} \qquad \text{(Eq. G.2)}$$

where **k**: position index (k = 1,…,m) and $\Delta\eta$ = 1/m. Eq. G.1 can be thus rewritten as Eq. G.3

$$P_i^k = P_i^{k-1}\left[1 - \alpha_i \frac{q_{M,i}}{q_i^{k-1} f\left(q_T^{k-1}\right)} \Delta\eta\right] \qquad \text{(Eq. G.3)}$$

Eq. G.3 is solved to calculate the **k** point for a set of initial values of the alpha-parameters. The partial pressures are calculated slab-wise, that is, the value of axial position **k** is varied from 1 to m. At each position **k**, the composition of each species **i** is calculated iteratively according to the scheme shown in Figure G.1. The set of alpha parameters are optimized by the least-square method using the Levenberg-Marquardt algorithm. Finally, Figure G.2 shows a scheme of the program used for carrying out the fittings of experimental data to the model.

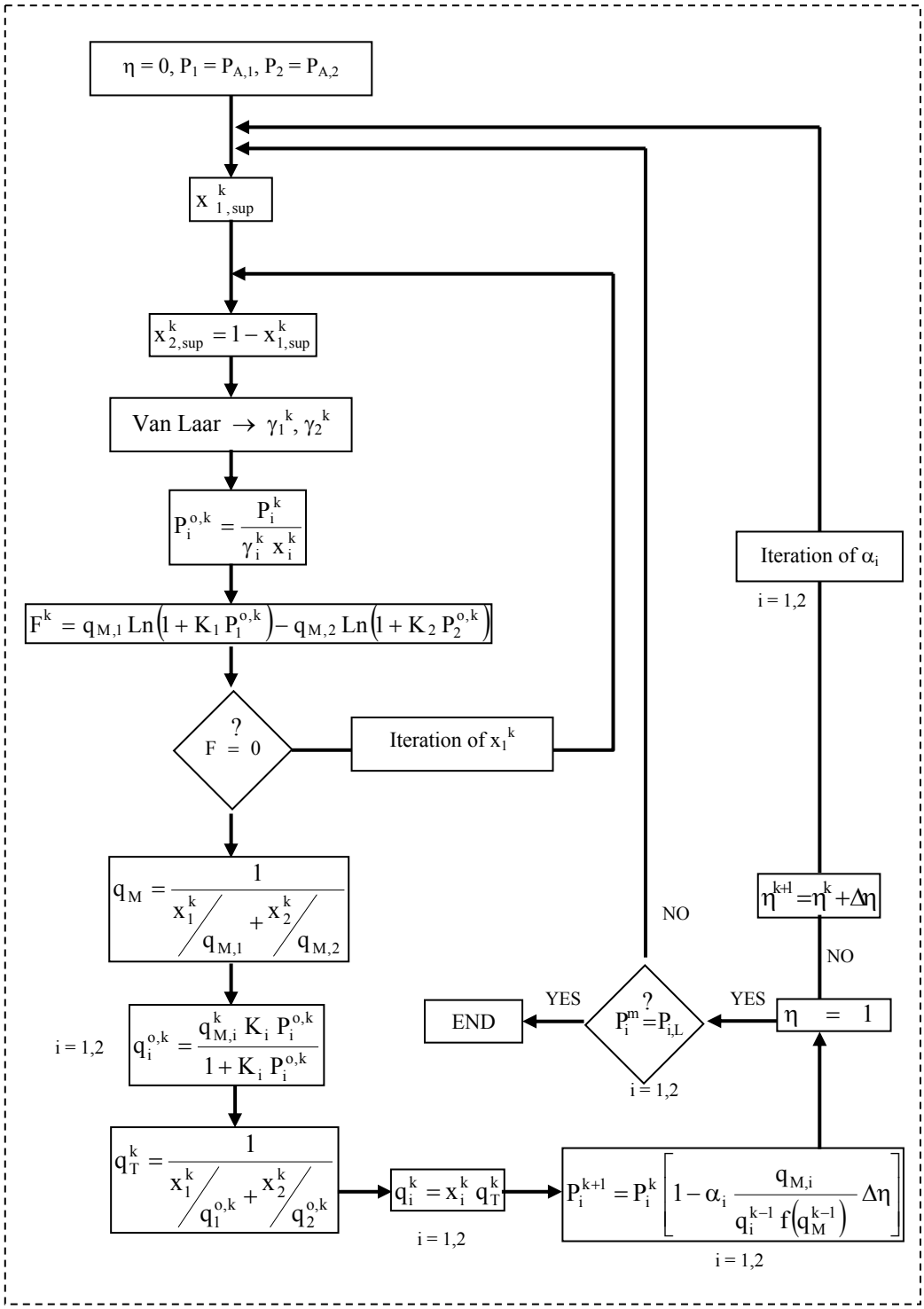

Figure G.1: Schematic representation of the procedure to determine alpha parameters that characterize the PV of both water and ethanol through a zeolite NaA membrane.

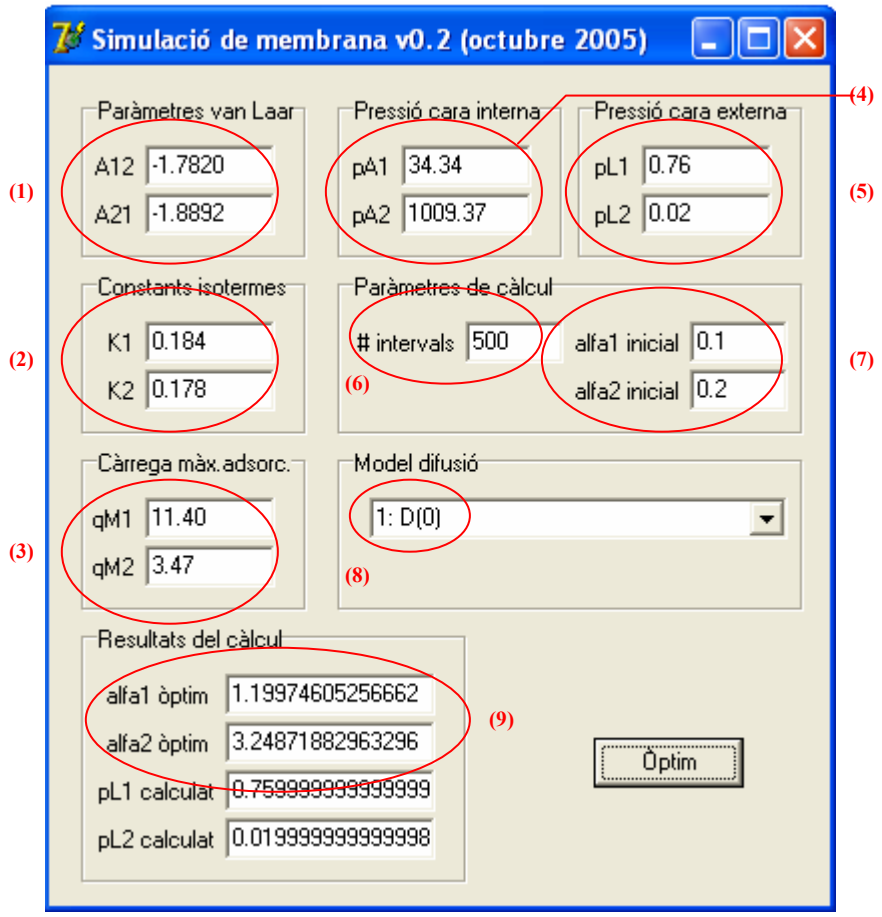

Figure G.2 Screen of the program used to optimize surface diffusivities from VPV data in zeolite NaA membranes using the PRAST approach. (1) Parameters of the Van Laar model [-], (2) Adsorption constants [$mmHg^{-1}$], (3) Molar saturation loadings [mol kg^{-1}], (4) Input data for partial pressures in the feed/membrane surface, (5) Input data for partial pressures in the membrane/permeate surface, (6) Number of finite elements in the thickness of the zeolite NaA layer, (7) Initial values for dimensionless surface fluxes, (8) Surface diffusivity model, (9) Optimized dimensionless surface fluxes.